

Widely tunable single-mode quantum cascade laser source for mid-infrared spectroscopy

Benjamin G. Lee,^{a)} Mikhail A. Belkin,^{b)} Ross Audet,^{c)} Jim MacArthur, Laurent Diehl, Christian Pflügl, and Federico Capasso^{d)}
School of Engineering and Applied Sciences, Harvard University, 9 Oxford Street, Cambridge, Massachusetts 02138, USA

Douglas C. Oakley, David Chapman, and Antonio Napoleone
Lincoln Laboratory, Massachusetts Institute of Technology, 244 Wood Street, Lexington, Massachusetts 02420, USA

David Bour,^{e)} Scott Corzine,^{f)} and Gloria Höfler^{g)}
Agilent Laboratories, 3500 Deer Creek Road, Palo Alto, California 94304, USA

Jérôme Faist
ETH Zurich, HPT H 7, Wolfgang-Pauli-Str. 16, 8093 Zürich, Switzerland

(Received 20 October 2007; accepted 2 November 2007; published online 3 December 2007)

We demonstrate a compact, single-mode quantum cascade laser source continuously tunable between 8.7 and 9.4 μm . The source consists of an array of single-mode distributed feedback quantum cascade lasers with closely spaced emission wavelengths fabricated monolithically on a single chip and driven by a microelectronic controller. Our source is suitable for a variety of chemical sensing applications. Here, we use it to perform absorption spectroscopy of fluids. © 2007 American Institute of Physics. [DOI: 10.1063/1.2816909]

Quantum cascade lasers (QCLs) are semiconductor lasers based on resonant tunneling and optical transitions between electronic levels within the conduction band of a multi-quantum well structure. As a result, the emitted photon energy is determined by the thicknesses of the wells and barriers and can be tailored by band-gap engineering. The emission wavelengths of mid-infrared QCLs span from 3 to 24 μm (Ref. 1) and cover the “fingerprint” region of molecular absorption. This makes QCLs particularly interesting for spectroscopic applications.^{2–6} QCLs can achieve output powers as large as hundreds of milliwatts in continuous wave operation at room temperature^{7,8} and can be designed with broadband gain, with full width at half maximum of more than 300 cm^{-1} , enabling wide wavelength tunability.⁹

In addition to a wide tuning range, single-mode emission is required for most spectroscopic applications. To achieve single-mode emission, QCL material is typically processed into distributed feedback (DFB) lasers^{10,11} or integrated with an external cavity (EC).^{9,12,13} EC QCLs are widely tunable but are cumbersome and complex to build. They require high quality antireflection coatings, well-aligned external optical components including a grating for tuning, and piezoelectric controllers. DFB QCLs are very compact, but a single DFB QCL has limited tunability, achieved by changing the temperature of the active region of a device, with a typical tuning coefficient of $\sim 0.07 \text{ cm}^{-1}/\text{K}$.¹⁰ In this letter, we present

a widely tunable, single-mode QCL source that combines the advantages of DFB QCLs and EC QCLs.

Our device is based on an array of DFB QCLs with closely spaced emission wavelengths spanning the gain bandwidth of the QCL material, fabricated monolithically on the same chip and driven individually by a microelectronic controller [Fig. 1(a)]. The spacing of the emission wavelengths of the lasers in the array is sufficiently small such

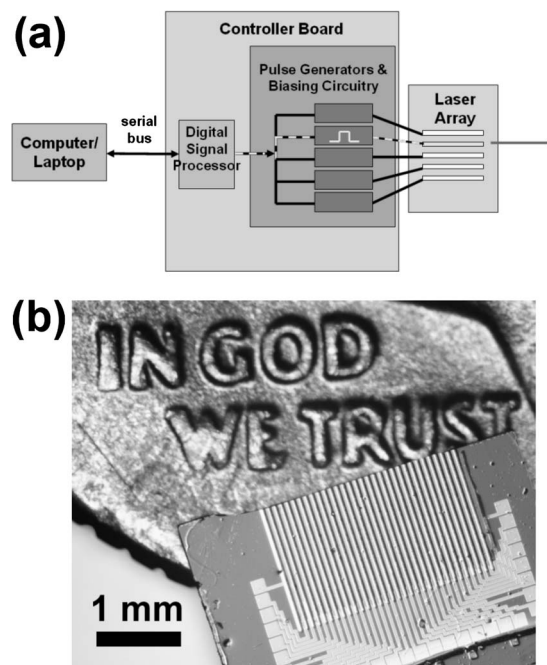


FIG. 1. (a) Schematic of the widely tunable quantum cascade laser source with a distributed feedback laser array driven by a custom microelectronic controller. The dotted line denotes the routing of the current pulse and the DC bias to a specific laser (second from top) to fire it at a specified wavelength. (b) The processed laser array chip placed on top of a dime for size comparison. Squares on the bottom portion of the chip are gold pads for wire bonding.

^{a)}Electronic mail: bglee@fas.harvard.edu.

^{b)}Electronic mail: mbelkin@seas.harvard.edu.

^{c)}Present address: Department of Electrical Engineering, Stanford University, 350 Serra Mall, Stanford, CA 94305.

^{d)}Electronic mail: capasso@seas.harvard.edu.

^{e)}Present address: Photodigm, Inc., 1155 E. Collins Blvd. No. 200, Richardson, TX 75081.

^{f)}Present address: Infinera HQ, 169 Java Dr., Sunnyvale, CA 94089.

^{g)}Present address: Argos Tech LLC, 3671 Enochs St., Santa Clara, CA 95051.

that for any wavelength within the gain spectrum of the QCL material, one can select a DFB QCL in the array and adjust its temperature to produce single-mode emission at the desired frequency. The custom-designed controller consists of pulse generators to power the lasers, direct current bias circuitry to heat individual lasers in the array for temperature tuning, and a serial port interface for computer control of laser firing.

The QCL material used to fabricate the laser array was grown by metalorganic vapor phase epitaxy (MOVPE). The structure consists of a bottom waveguide cladding of $4\ \mu\text{m}$ of InP doped $1 \times 10^{17}\ \text{cm}^{-3}$, followed by $580\ \text{nm}$ of InGaAs doped $3 \times 10^{16}\ \text{cm}^{-3}$, a $2.4\text{-}\mu\text{m}$ -thick lattice-matched active region, $580\ \text{nm}$ of InGaAs doped $3 \times 10^{16}\ \text{cm}^{-3}$, and a top waveguide cladding consisting of $4\ \mu\text{m}$ of InP doped $1 \times 10^{17}\ \text{cm}^{-3}$ and $0.5\ \mu\text{m}$ of InP doped $5 \times 10^{18}\ \text{cm}^{-3}$. The active region consists of 35 stages based on a bound-to-continuum design emitting at $\sim 9\ \mu\text{m}$.¹³

Device processing started with the fabrication of an array of 32 buried DFB gratings in the QCL material. Grating periods ranged between 1.365 and $1.484\ \mu\text{m}$, satisfying the Bragg condition for lasing wavelengths between 8.63 and $9.38\ \mu\text{m}$, assuming an effective refractive index of 3.16 . To fabricate the buried gratings, the top waveguide cladding was removed down to the first InGaAs layer, using concentrated HCl as a selective wet etch. Then, a 200-nm -thick layer of Si_3N_4 was deposited on top of the InGaAs by chemical vapor deposition. First-order Bragg gratings were exposed onto AZ-5214 image-reversal photoresist by optical lithography, using a photomask where the grating patterns had been defined by electron-beam writing. This pattern was transferred into the Si_3N_4 by using a CF_4 -based dry etch. The gratings were then etched $500\ \text{nm}$ deep into the top InGaAs layer with a $\text{HBr}/\text{BCl}_3/\text{Ar}/\text{CH}_4$ plasma in an inductively coupled plasma reactive ion etching machine (ICP-RIE). The InP top cladding was re-grown over the gratings using MOVPE. The grating coupling strength was calculated using coupled wave theory¹⁴ to be $\kappa \sim 30\ \text{cm}^{-1}$.

Laser ridges, $15\text{-}\mu\text{m}$ -wide and spaced $75\ \mu\text{m}$ apart, were defined on top of the buried gratings by dry etching the surrounding areas $9\ \mu\text{m}$ deep with a $\text{HBr}/\text{BCl}_3/\text{Ar}/\text{CH}_4$ plasma using ICP-RIE. During this step, the back facet of the lasers was also defined. The bottom and the sidewalls of the laser ridges were insulated by Si_3N_4 and a 400-nm -thick gold top contact was deposited. The samples were then thinned to $200\ \mu\text{m}$ and a metal bottom contact was deposited. Finally, the front facets of the lasers were defined by cleaving to obtain 3.5-mm -long lasers and the laser array was indium soldered onto a copper block for testing. The facets were left uncoated. The entire DFB laser array chip is only $4 \times 5\ \text{mm}^2$ in size [Fig. 1(b)].

For testing, all 32 lasers in the array were individually wire bonded to a circuit board, which was connected to the custom-built controller. The lasers were tested in pulsed mode with $40\ \text{ns}$ pulses at a repetition rate of $100\ \text{kHz}$ at room temperature. We demonstrated individual addressing and firing of the lasers in arbitrary order using the computer-controlled electronics. All 32 lasers in the array operated single mode [Fig. 2(a)]. The lasing frequencies of the QCLs in the array were spaced $\sim 2.75\ \text{cm}^{-1}$ apart and spanned from 1146 to $1061\ \text{cm}^{-1}$ (8.73 to $9.43\ \mu\text{m}$). Subthreshold measurements revealed the bandgap of the DFB grating to be

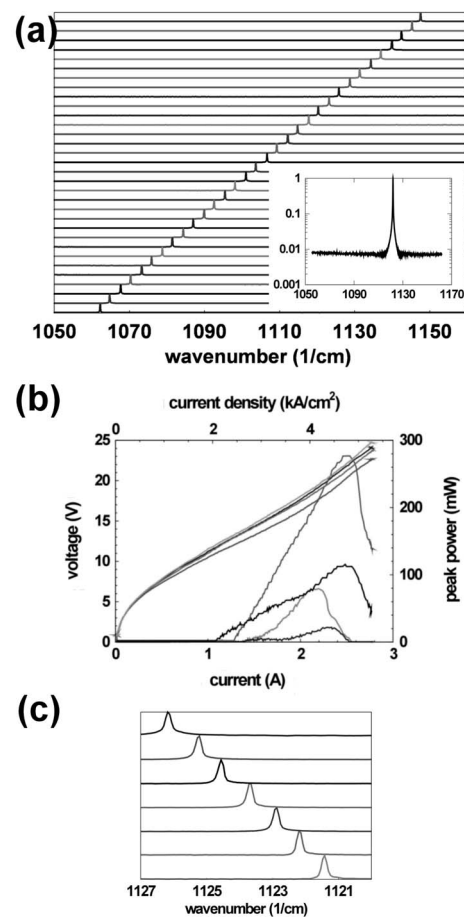


FIG. 2. (a) Spectra of 32 single-mode distributed feedback lasers in the array. Laser frequencies are spaced $\sim 2.75\ \text{cm}^{-1}$ apart and span a range of $\sim 85\ \text{cm}^{-1}$. (Inset) Spectrum of a representative laser in the array on a log scale, showing side-mode suppression $>20\ \text{dB}$. (b) Plot of the voltage (left axis) and light output (right axis) characteristics of several representative lasers in the array as functions of current. (c) Temperature tuning of the emission frequency of a laser in the array by heating it from 300 to $390\ \text{K}$ in 15° increments (traces arranged top to bottom, respectively).

$3.1\ \text{cm}^{-1}$, giving a coupling strength $\kappa \approx 31\ \text{cm}^{-1}$, in agreement with our calculations.

Threshold currents for the DFB lasers in the array ranged from 1.1 to $1.3\ \text{A}$, corresponding to current densities of 2.1 and $2.5\ \text{kA}/\text{cm}^2$ [Fig. 2(b)], with lower values observed for the lasers with emission frequency near the center of gain. All the DFB lasers remained single mode with $>20\ \text{dB}$ side-mode suppression up to at least $1.8\ \text{A}$ in current [Fig. 2(a), inset]. There were small differences in the I - V curves of the lasers resulting from the varying series resistances of different length gold contacts running between the laser ridges and the wirebond pads on the QCL array chip. We also observed an unexpectedly large variation in the slope efficiency of the lasers between 20 and $200\ \text{mW}/\text{A}$.

The variation in slope efficiency is not correlated with the scatter in threshold current density, and is likely due to the random variation in the position of the end mirror facets relative to the laser ridge gratings. As shown in Ref. 15, the variation in the position of the laser facet alters the distribution of light intensity within the laser cavity, which results in a variation in the amount of light emitted from a facet. We further note that our DFB lasers operate in the over-coupled regime ($\kappa L = 11$) and that current injection into the ridges is nonuniform because of the voltage drop along the laser ridge caused by the resistance ($\sim 5\ \Omega$) of the metal contact over

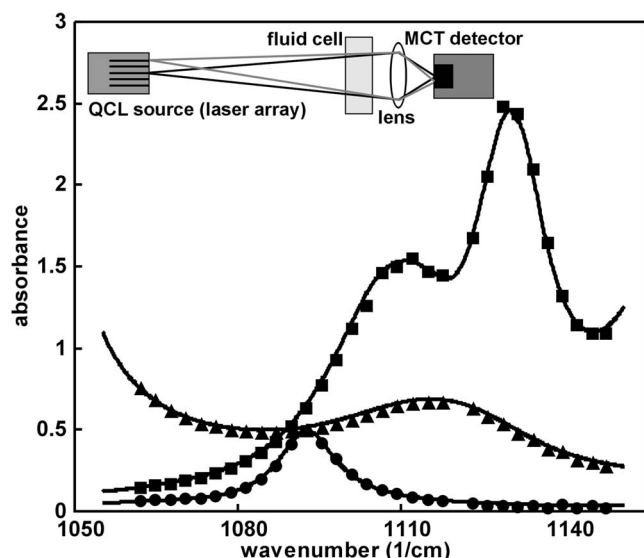


FIG. 3. Absorption spectra of isopropanol (squares), methanol (triangles), and acetone (circles) obtained with the laser array and with a Bruker Vertex 80v Fourier transform infrared spectrometer (continuous lines). (Inset) Experimental setup for mid-infrared spectroscopy of liquids with the quantum cascade laser source.

the length of the ridge. These two factors, the strong coupling and the inhomogeneous current injection, can result in a highly nonuniform profile of the light intensity inside the laser ridge and may also be responsible for the observed variation in slope efficiencies. We also believe, however, that these effects and the presence of a small amount of loss coupling ($\sim 0.1 \text{ cm}^{-1}$) are the reason for the mode selection in our DFB lasers, as all our lasers consistently operate in the antisymmetric DFB mode. We will further explore these effects in future work.

To obtain continuous spectral coverage, individual DFB QCLs in the array must be temperature tuned to cover gaps between the nominal frequencies of two adjacent lasers. This can be done by heating the lasers with a (subthreshold) DC bias current or by changing the heatsink temperature. In Fig. 2(c), we demonstrate frequency tuning of an individual laser in the array by heating the laser from 300 to 390 K on a thermoelectric cooler/heater.

After calibration of the laser emission frequencies, our QCL source can be used for a variety of spectroscopic applications. Here, we demonstrate its application for mid-infrared absorption spectroscopy of liquids. Our setup consisted of the QCL source, a transparent BaF_2 fluid cell (23.6 μm chamber thickness) containing the analyte, and a mercury cadmium telluride liquid-nitrogen cooled detector [Fig. 3, inset]. A single lens, 12 mm in diameter and with a 12 mm focal length, was used to image the 2.5-mm-wide QCL array onto the $0.25 \times 0.25 \text{ mm}^2$ active area of the detector. To take a spectrum, the lasers were fired sequentially and the intensities of the transmitted beams were recovered from the detector using a gated integrator. One of the lasers was damaged during handling so only 31 out of the 32 lasers were used. After taking the background and sample spectra, we obtained the absorption spectrum using a frequency table

with data for each laser in the array [Fig. 3]. It took us approximately 10 s to obtain each spectrum. Our results compare favorably with spectra obtained using a conventional Fourier transform infrared (FTIR) spectrometer, also shown in Fig. 3. We note that the frequency resolution of our QCL source is determined by the lasers' linewidths, which were measured to be $\sim 0.01 \text{ cm}^{-1}$ in pulsed operation and $< 0.001 \text{ cm}^{-1}$ in continuous-wave operation.¹⁰ This is significantly better than the resolution offered by a typical "bench-top" FTIR ($\sim 0.1 \text{ cm}^{-1}$). Despite the narrower spectral measurement range compared to FTIR spectrometers, we believe that a spectrometer based on our QCL source can provide a portable alternative to FTIR spectrometers in the mid-infrared molecular fingerprint region.

Several development steps are left for future work. At present, the separate beams emerging from the individual lasers in the array are not combined into a single beam. Future work will include developing a tapered waveguide or other beam combining scheme to combine and collimate laser beams emitted from the QCL array into a single output. We also aim to increase the spectral coverage of the QCL source to more than 200 cm^{-1} . We hope to integrate our source into a variety of spectroscopic devices, including a portable spectrometer operating in the mid-infrared molecular fingerprint region.

The authors acknowledge funding support from the DARPA Optofluidics Center under Grant No. HR0011-04-1-0032. The Center for Nanoscale Systems (CNS) at Harvard University is also gratefully acknowledged. Harvard-CNS is a member of the National Nanotechnology Infrastructure Network (NNIN).

¹F. Capasso, C. Gmachl, D. L. Sivco, and A. Y. Cho, *Phys. Today* **55**(5), 34 (2002).

²A. Kosterev and F. Tittel, *IEEE J. Quantum Electron.* **38**, 582 (2002).

³C. Charlton, F. de Melas, A. Inberg, N. Croitoru, and B. Mizaikoff, *IEE Proc.: Optoelectron.* **150**, 306 (2003).

⁴D. D. Nelson, J. H. Shorter, J. B. McManus, and M. S. Zahniser, *Appl. Phys. B: Lasers Opt.* **75**, 343 (2002).

⁵S. Schaden, A. Domínguez-Vidal, and B. Lendl, *Appl. Phys. B: Lasers Opt.* **86**, 347 (2007).

⁶M. A. Belkin, M. Lončar, B. G. Lee, C. Pflügl, R. Audet, L. Diehl, F. Capasso, D. Bour, S. Corzine, and G. Höfler, *Opt. Express* **15**, 11262 (2007).

⁷M. Beck, D. Hofstetter, T. Aellen, J. Faist, U. Oesterle, M. Ilegems, E. Gini, and H. Melchior, *Science* **295**, 301 (2002).

⁸L. Diehl, D. Bour, S. Corzine, J. Zhu, G. Höfler, M. Lončar, M. Troccoli, and F. Capasso, *Appl. Phys. Lett.* **88**, 201115 (2006).

⁹R. Maulini, A. Mohan, M. Giovannini, J. Faist, and E. Gini, *Appl. Phys. Lett.* **88**, 201113 (2006).

¹⁰C. Gmachl, A. Straub, R. Colombelli, F. Capasso, D. L. Sivco, A. M. Sergent, and A. Y. Cho, *IEEE J. Quantum Electron.* **38**, 569 (2002).

¹¹A. Wittmann, M. Giovannini, J. Faist, L. Hvozďara, S. Blaser, D. Hofstetter, and E. Gini, *Appl. Phys. Lett.* **89**, 141116 (2006).

¹²G. Wysocki, R. F. Curl, F. K. Tittel, R. Maulini, J. M. Bulliard, and J. Faist, *Appl. Phys. B: Lasers Opt.* **81**, 769 (2005).

¹³R. Maulini, M. Beck, J. Faist, and E. Gini, *Appl. Phys. Lett.* **84**, 1659 (2004).

¹⁴H. Kogelnik and C. V. Shank, *J. Appl. Phys.* **43**, 2327 (1972).

¹⁵W. Streifer, R. Burnham, and D. Scifres, *IEEE J. Quantum Electron.* **11**, 154 (1975).